Downloaded 10/14/16 to 128.114.69.142. Redistribution subject to SEG license or copyright; see Terms of Use at http://library.seg.org/

Reflected wave least-squares migration with correct image phase

Huamin Zhou[1,2], Shengchang Chen[1], Rushan Wu[2], Xiaobi Xie[2], , Haoran Ren[1], 1. Zhejiang University, China. 2. University of California, santa cruz

Summary

Least squares migration is regraded as one of the best image method for its capable of suppressing migration artifacts, balancing amplitude and improving resolution. This paper proposes a least squares reverse time migration (LSRTM) with correct phase information scheme for seeking a stacked reflectivity model. The second type Rayleigh integral is used to accurately reconstruct the local scattered wavefield and simulate reflected demigration data in LSRTM. With this, both the image and demigration data have the correct phase information. A source-receiver combined illumination and a first spatial derivative regularization term are used to accelerate the convergence. The numerical test successfully demonstrates that this LSRTM scheme can gain images with correct phase, balanced amplitude, broader bandwidth and high resolution. The obtained image can be used as an estimation of the subsurface's reflectivity.

Introduction

Least squares migration (LSM) tries to iteratively seek a stacked reflectivity model so as to best match the observed seismic data in least squares sense. Unlike conventional migration, who replaces the inverse with the adjoint operator of the forward modeling, LSM is a linear seismic inversion method with the goal of gaining an image of balanced amplitude and high resolution.

After proposed by Tarantola(1984), LSM has developed from least squares Kirchhoff migration (Nemeth, et al., 1999) to one-way wave equation LSM (Kuhl, et al.,2003; Zhou,2014) and recently to least squares reverse time migration. LSRTM is considered to be one of the best imaging methods, as it combines the advantage of inversion method and high precision full wave equation (Zhang, 2015). Generally, people focus on improving the efficiency of LSRTM, such as phase encoding or preconditioning method(Tang, 2009;Dai, 2010). However, in most of those LSRTM studies, an image of the velocity contrast is inverted instead of reflectivity. So the image result is not the reflectivity and the phase of the image is inaccurate. In order to gain the correct image, an essential step is to eliminate the propagation effects by means of wave-field extrapolation. In reflection seismic theory, Kirchhoff integral is the mathematic discription of the propagation of seismic wave. When the surface is a plane surface, it can be simplified to the first and second type Rayleigh integral, which helps to accelerate the calculation of the propagation of the wavefield (Berkhout, 1989，Keho,1988). The true-amplitude migration on the basis of Kirchhoff migration has been extensively studied(Bleistein,1987). But using ray tracing to approximate the Green's function may compromise the accuracy of Kirchhoff migration. The RTM method (Baysal,1983), with the use of the two-way wave equation to calculate Green's function, can better maintain the amplitude information during propagation.

In this paper, we propose a reflected wave least squares reverse time migration with accurate phase image method. Firstly, we use the second type Rayleigh integral (RI) to reconstruct the receiver wavefield as an initial problem, this is crucial to regain the true phase information of the reverse time propagated wavefield. With this Rayleigh propagator, the linear demigration and migration of reflected seismic data can gain correct phase and amplitude of the local scattered wavefield. Then by LSRTM, we can obtain a high quality image for reflectivity estimation . A source-receiver combined illumination and regularization are used to speed up the convergence. Numerical test demonstrates that this LSRTM scheme can obtain images with correct phase, balanced amplitude, broader bandwidth and high resolution.

Theory

For a survey system composed of a shot at x_s and receiver at x_g , reflected seismic data recorded on the surface can be expressed as:

$$d(\boldsymbol{x}_g, \boldsymbol{x}_s, \omega) = f(\omega)\int_v G(\boldsymbol{x}', \boldsymbol{x}_s, \omega)m(\boldsymbol{x}')G(\boldsymbol{x}', \boldsymbol{x}_g, \omega)d\boldsymbol{x} \quad (1)$$

where ω is the angular frequency, $f(\omega)$ is the wavelet in the frequency domain, $G(x'; x_s; \omega)$ is the Green's function from shot to reflector at x' ; $G(x'; x_g; \omega)$ is the Green's function from reflector to receiver. $m(\boldsymbol{x}')$ is the reflectivity model. $d(x_g; x_s; \omega)$ is the seismic data. Generally, migration contains forward propagation of the source wavefield and backward propagation of the receiver wavefield by reducing time, then applys imaging condition to gain the subsurface's image result. So the precise reconstruction of the backpropagated wavefield plays an important role in seismic migration. Kirchhoff integral is an exact mathematic formula for describing wave propagation. In exploration seismology, the recorded wavefield usually is measured on the surface, so if the surface is a plane surface,

© 2016 SEG

Downloaded 10/14/16 to 128.114.69.142. Redistribution subject to SEG license or copyright; see Terms of Use at http://library.seg.org/

Kirchhoff integral can be simplified to the widely used second type Rayleigh integral,

$$u(\boldsymbol{x},\boldsymbol{x}_g,\omega)=-2\oint_S d(\boldsymbol{x}_g,\boldsymbol{x}_s,\omega)\frac{\partial G^*(\boldsymbol{x},\boldsymbol{x}_g,\omega)}{\partial n}dS(\boldsymbol{x}) \quad (2)$$

where $*$ is the adjoint operator, $u(\boldsymbol{x},\boldsymbol{x}_g,\omega)$ is the backpropagated wavefield from receiver to image point at x, $\partial G/\partial n$ is the normal derivative of the Green function, n is the normal vector of the recording surface. In the wavenumber domain, equation (2) also can be written as,

$$u(\boldsymbol{x},\boldsymbol{x}_g,k_x;\omega)=2\oint_S ik_z d(\boldsymbol{x}_g,\boldsymbol{x}_s,k_x;\omega)G(\boldsymbol{x},\boldsymbol{x}_g,k_x;\omega)dS(\boldsymbol{x}) \quad (3)$$

where k_z is the vertical wavenumber, it also can be expressed as $k_z = k\cos\theta$, k is the wavenumber of the propagated direction, θ is the angle of backpropagated wave and z-axis. By applying the second type Rayleigh integral, backpropagated wavefield can accurately reconstruct the phase and traveltime information of the reflected wave. Then migration can be formed as the crosscorrelation between backward receiver wavefield and forward source wavefield,

$$I(\boldsymbol{x})=\sum_{\omega}\sum_{x_s} f(\omega)G^*(\boldsymbol{x},\boldsymbol{x}_s,\omega)\sum_{x_g}u(\boldsymbol{x},\boldsymbol{x}_g,\omega) \quad (4)$$

The second type Rayleigh operator help reverse time migration to obtain an image with correct phase and waveform infromation. But from equation (4), it is obvious that RTM replaces the inversed operator with its adjoint operator. So the migration image may suffers from distortion, low resolution because of the limit geometry, complex geological structures or other restriction in seismic exploration. Then the RTM image result can be view as a blurry version of the true reflectivity model. To furter gain a true amplitude image, least squares migration is applied. The objective function of the constrained regularization least square migration is,

$$F\left(m(\boldsymbol{x})\right)=\frac{1}{2}\left\|d(\boldsymbol{x}_g,t)-Lm(\boldsymbol{x})\right\|^2+\frac{\lambda}{2}\left\|\frac{\partial m(\boldsymbol{x})}{\partial \boldsymbol{x}}\right\|^2 \quad (5)$$

The first term is the residual term, the second term is the regularization term, which can be expressed as the first spatial derivatives of the image. λ the weighting factor of these two terms. L is the linear forward modeling operator. From equation (3) and (4), this linear forward modeling $Lm(\boldsymbol{x})$ can be expressed as,

$$Lm(\boldsymbol{x})=\sum_{\omega}\sum_{x_s} f(\omega)ik_z G(\boldsymbol{x},\boldsymbol{x}_s,k_x,\omega)m(\boldsymbol{x})G(\boldsymbol{x},\boldsymbol{x}_g,k_x;\omega) \quad (6)$$

In order to speed up the convergence rate of the iteration, a source-receiver combined illumination can be used as a preconditioner,

$$\widehat{H}(\boldsymbol{x})=\sum_{\omega}\sum_{x_s} f^2(\omega)ik_z G(\boldsymbol{x},\boldsymbol{x}_s,k_x,\omega)G^*(\boldsymbol{x},\boldsymbol{x}_s,k_x,\omega) \times\sum_{\boldsymbol{x}_g}G(\boldsymbol{x},\boldsymbol{x}_g,k_x;\omega)G^*(\boldsymbol{x},\boldsymbol{x}_g,k_x;\omega) \quad (7)$$

Then the update of the LSRTM result can be implemented as,

$$m_{k+1}=m_k+\alpha_k\widehat{H}^{-1}\left(L^*(d-Lm_k)+\lambda R_k\right) \quad (8)$$

Where subscript k^{th} indicates iterative times, α is the iterative step length, and can be obtained by linear search method.

Exmaple

To test the effectiveness of the proposed method, part of the Sigsbee2a velocity model was extracted. the model size is 6km x3km with 10m x10m grid interval. 300 shots were fired with 10m shot interval . Synthetic data are generated by a finite difference solver with a 18-Hz Ricker wavelet; the recording length is 4s.

Figure 1(a) is the theoretical reflectivity model calculated by vertical reflectivity, figure 1(b) is the conventional migration result, figure 1(c) is the RTM result using equation (4), and figure 1(d) is the LSRTM result after 10 iterations. From those migration result, we can see that LSRTM show high imaging quality than conventional RTM result. LSRTM can improve the energy in the deep part of the model. The image in figure1(d) is closer to the real reflectivity model in figure 1(a). The overall performance is shown with more balanced amplitude, improved resolution. Compared the RTM result of (b) and (c), we can see that conventional reverse time migration can't precisely image the subsurface's structure since the phase and waveform in figure1(b) didn't match well with the theoretical reflectivity model. In comparison, the image's waveform in figure 1(c) and (d) agree well with that in figure 1(a).

To compare those image's waveform in detail, we plot the vertical profiles of figure 1a, b, c and d at x=3 km (the red line in figure1a) and shown in figure 2. Figure 2(a) and (b) are respectively the shallow and deep part of this profile. The black solid line is the theoretical reflectivity. Green dashed line, blue dashed line and red solid line are respectively the result of conventional RTM, RTM with the use of RI operator and the LSRTM with the use of RI operator. From this profile, we can see that conventional RTM suffers from a phase shift, thus the waveform and the phase didn't match the theoretical waveform. While RTM with the Rayleigh operator can avoid this problem. Its waveform is similar to the Ricker wavelet whose peak amplitude corresponds to the reflector's location. But RTM's amplitude is not accurate. While LSRTM, as a

© 2016 SEG

Downloaded 10/14/16 to 128.114.69.142. Redistribution subject to SEG license or copyright; see Terms of Use at http://library.seg.org/

linear inversion method, can enhance the total energy of the image, especially the deep part. Its amplitude is closer to the therotical value. What's more, LSRTM tries to compensate for the source signature to obtain the true reflectivity, so its image has weaker side lobes and high resolution.

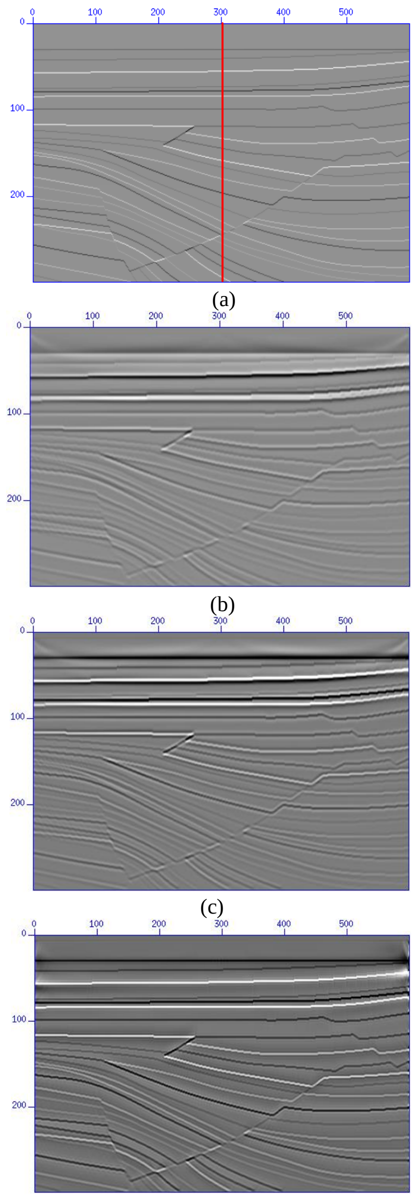

Figure1. true reflectivity model (a), conventional RTM result (b), RTM with the use of RI propagator (c) and LSRTM result with the use of RI propagator (d)

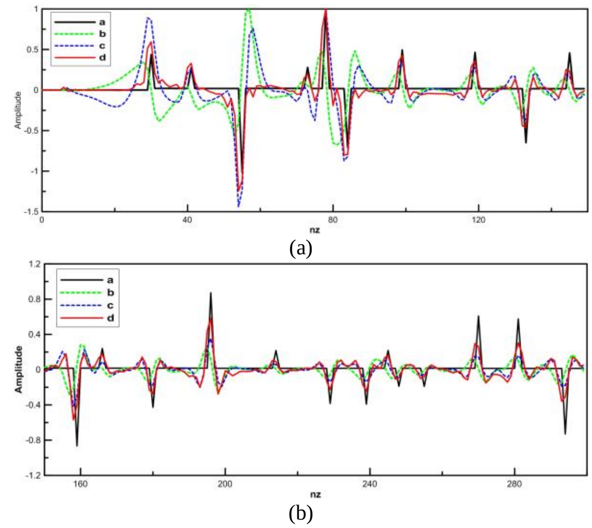

Figure 2. the profile of a trace at 3km extracted from figure 1. a,b,c,d. (a) depth from 0 to 1.5km, (b) depth from 1.5km to 3km.

From this test, we can see that LSRTM image has higher resolution than RTM. Furthermore, the amplitudes of LSRTM image are more balanced, which are closer to the true value. Figure 3 compares the demigration data of LSRTM vcand RTM result. It shows that LSRTM can better approximate the observed data, and recover some weakly reflected waveform in the deep reflector. Even though LSRTM tries to fit the observed data by improving the fidelity of the image result, the demigrated data can't fully match the recorded data, as those two methods are generated in different ways.

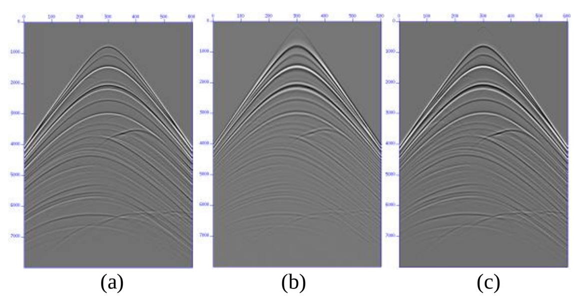

Figure 3 seismic data(a), demigration data with RTM result(b), demigration data with LSRTM result(c).

In the second example, we apply this LSRTM method to the standard Marmousi model data. The size of the model is 343x750 grid. 240 shots are excited with a 25-m shot interval. Each shot has 96 receivers. The source is a 25-Hz peak frequency Ricker wavelet, and the recording time length is 3 s.

Figure 4 shows the RTM result using this paper's method and its corresponding LSRTM result after 12 iterations. It is obvious that even thought our RTM method can gain much better imaging result, it still encounters imaging distribution problem. Especially for the high velocity anticline part, the events appear to be discontinuous. While the LSRTM result with 12 iterations can obviously enhance the balance of the imaging amplitude. The image of the shallow part has high resolution and better continuity. Energy losing phenomenon due to the three overlying shallow faults and middle anticline is significantly improved, thus highlighting the deep local structures. The overall Figure4(b) has more balanced energy, improved resolution and high image quality.

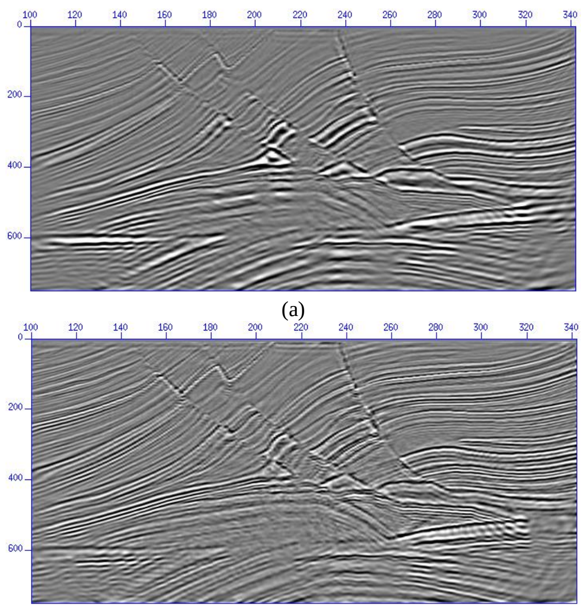

(a)

(b)

Figure 4. RTM result(a) and LSRTM result (b)

Conculusion

A least-square reverse time migration method with correct image phase information was proposed for iteratively seeking a stacked reflectivity model. With the use of second type Rayleigh integral, migration and demigration can precisely reconstruct the backpropagated wavefield and generate the corresponding reflected wavefield. This makes migration and least squares migration have correct phase information and the image is closer to the real reflectivity model. To accelerate the convergence rate, a first-order spatial derivative of the image is used as a regularization term and the subsurface two-way illumination is used as a preconditioner. Applying this reflected wave least squares migration method to synthetic data proves that it can suppress the side lobes and artifacts of the image, remove the high wavenumber noise and expand the bandwidth. Therefore produce an image with high resolution, balanced amplitude, so that it can be used as an estimation of the subsurface's reflectivity model.

Acknowledgments

We greatly appreciate the support of the Natural Science Foundation of China (41374001, 41304089) and the WTOPI Research Consortium at the University of California, Santa Cruz.

Downloaded 10/14/16 to 128.114.69.142. Redistribution subject to SEG license or copyright; see Terms of Use at http://library.seg.org/

© 2016 SEG

EDITED REFERENCES

Note: This reference list is a copyedited version of the reference list submitted by the author. Reference lists for the 2016 SEG Technical Program Expanded Abstracts have been copyedited so that references provided with the online metadata for each paper will achieve a high degree of linking to cited sources that appear on the Web.

REFERENCES

Baysal, E., D. Kosloff, and J. W. C. Sherwood, 1983, Reverse time migration: Geophysics, **48**, 1514–1524, http://dx.doi.org/10.1190/1.1441434.

Berkhout, A. J., and C. P. A. Wapenaar, One-ways version of the Kirchhoff integral: Geophysics, **54**, 460–467, http://dx.doi.org/10.1190/1.1442672.

Bleistein, N., 1987, On the imaging of reflectors in the earth: Geophysics, **52**, 931–942, http://dx.doi.org/10.1190/1.1441970.

Chen, S.-C., and H.-M. Zhou, 2016, Re-exploration to migration of seismic data (in Chinese): Chinese Journal of Geophysics, **59**, 54–67, http://dx.doi.org/10.1002/cjg2.20213.

Dai, W., C. Boonyasiriwat, and G. T. Schuster, 2010, 3D multi-source least-squares reverse time migration: 80th Annual International Meeting, SEG, Expanded Abstracts, 3120–3124.

Keho, T. H., and W. B. Beydoun, 1988, Paraxial ray Kirchhoff migration: Geophysics, **53**, 1540–1546, http://dx.doi.org/10.1190/1.1442435.

Kühl, H., and M. Sacchi, 2003, Least-squares wave-equation migration for AVP/AVA inversion: Geophysics, **68**, 262–273, http://dx.doi.org/10.1190/1.1543212.

Nemeth, T., C. Wu, and G. T. Schuster, 1999, Least-squares migration of incomplete reflection data: Geophysics, **64**, 208–221, http://dx.doi.org/10.1190/1.1444517.

Tang, Y., and B. Biondi, 2009, Least-squares migration/inversion of blended data: 79th Annual International Meeting, SEG, Expanded Abstracts, 2859–2863.

Tarantola, A., 1984, Inversion of seismic reflection data in the acoustic approximation: Geophysics, **49**, 1259–1266, http://dx.doi.org/10.1190/1.1441754.

Zhang, Y., L. Duan, and Y. Xie, 2015, A stable and practical implementation of least-square reverse time migration: Geophysics, **80**, no. 1, V23–V31, http://dx.doi.org/10.1190/geo2013-0461.1.

Zhou, H.-M., S.-C. Chen, H.-R. Ren, H.-C. Wang, and G.-X. Chen, 2014, One-way wave equation least-squares migration based on illumination compensation (in Chinese): Chinese Journal of Geophysics, **57**, 2644–2655, http://dx.doi.org/10.1002/cjg2.20136.

Downloaded 10/14/16 to 128.114.69.142. Redistribution subject to SEG license or copyright; see Terms of Use at http://library.seg.org/